Journal of Hazardous Materials 469 (2024) 134030

Contents lists available at ScienceDirect

Journal of Hazardous Materials

journal homepage: www.elsevier.com/locate/jhazmat

Research Paper

In vitro cell-transforming potential of secondary polyethylene terephthalate and polylactic acid nanoplastics

Josefa Domenech [a], Aliro Villacorta [b,c], Juan Francisco Ferrer [d], Raquel Llorens-Chiralt [d], Ricard Marcos [b], Alba Hernández [b], Julia Catalán [a,e,*]

[a] Finnish Institute of Occupational Health, Box 40, Työterveyslaitos, 00032 Helsinki, Finland
[b] Grup de Mutagènesi, Departament de Genètica i de Microbiologia, Facultat de Biociències, Universitat Autònoma de Barcelona, Bellaterra, Spain
[c] Facultad de Recursos Naturales Renovables, Universidad Arturo Prat, Iquique, Chile
[d] AIMPLAS, Plastics Technology Center, Valencia Parc Tecnologic, 46980 Paterna, Spain
[e] Department of Anatomy, Embryology and Genetics, University of Zaragoza, 50013 Zaragoza, Spain

HIGHLIGHTS

- Polyethylene terephthalate, polylactic acid, and polystyrene nanoplastics were used.
- Carcinogenicity was assessed using the *in vitro* Bhas 42 cell transformation assay.
- Only polyethylene terephthalate (PET) nanoplastics induced cell transformation.
- PET nanoplastics acted through a tumour promotion mode of action.
- The three types of nanoplastics were efficiently internalised into cells.

GRAPHICAL ABSTRACT

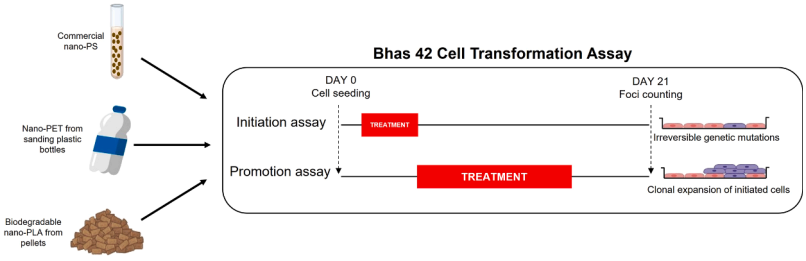

ARTICLE INFO

Keywords:
Polyethylene terephthalate
Polylactic acid
Polystyrene
Nanoplastics
Cell transformation

ABSTRACT

Continuous exposure to plastic pollutants may have serious consequences on human health. However, most toxicity assessments focus on non-environmentally relevant particles and rarely investigate long-term effects such as cancer induction. The present study assessed the carcinogenic potential of two secondary nanoplastics: polyethylene terephthalate (PET) particles generated from plastic bottles, and a biodegradable polylactic acid material, as respective examples of environmentally existing particles and new bioplastics. Pristine polystyrene nanoplastics were also included for comparison. A broad concentration range (6.25–200 μg/mL) of each nanoplastic was tested in both the initiation and promotion conditions of the regulatory assessment-accepted *in vitro* Bhas 42 cell transformation assay. Parallel cultures allowed confirmation of the efficient cellular internalisation of the three nanoplastics. Cell growth was enhanced by polystyrene in the initiation assay, and by PET in both conditions. Moreover, the number of transformed foci was significantly increased only by the highest PET concentration in the promotion assay, which also showed dose-dependency, indicating that nano PET can act as a non-genotoxic tumour promotor. Together, these findings support the carcinogenic risk assessment of nanoplastics and raise concerns regarding whether real-life co-exposure of PET nanoplastics and other environmental pollutants may result in synergistic transformation capacities.

* Corresponding author at: Finnish Institute of Occupational Health, Box 40, Työterveyslaitos, 00032 Helsinki, Finland.
E-mail address: julia.catalan@ttl.fi (J. Catalán).

https://doi.org/10.1016/j.jhazmat.2024.134030
Received 8 December 2023; Received in revised form 28 February 2024; Accepted 12 March 2024
Available online 13 March 2024

1. Introduction

The widespread use and disposal of plastic materials into the environment in recent decades has resulted in the emergence of micro- and nanoplastic pollution as a major concern for environmental safety and human health. The amount of plastic waste generated worldwide will reach 400 million metric tons in 2024 and is expected to triple by 2060, with recycling accounting for less than 20 % [74]. Secondary nanoplastics (NPLs) generated through the degradation and fragmentation of plastic waste are ubiquitous in all environmental niches, making human exposure through different routes (inhalation, oral, and dermal) unavoidable [27,28,53,66]. Moreover, owing to their size, NPLs can easily be internalised, resulting in a risk greater than that of microplastics. Nevertheless, few studies have assessed the effect of NPLs on human health. Of these, most describe acute effects, whereas long-term effects have been rarely explored, despite their considerable relevance owing to the high persistence and bioaccumulation of NPLs in different human tissues [13,27]. Furthermore, most research to date has used commercially available primary polystyrene (PS) nanoparticles (assessed in 70–80 % of all studies) instead of more environmentally relevant secondary NPLs [12,61,84]. In fact, the most common plastic polymers produced worldwide are polyethylene (26.3 %), polypropylene (18.9 %), polyvinyl chloride (12.7 %), and polyethylene terephthalate (6.2 %), whereas PS accounts for only 5.2 % of global production [31]. Similarly, little information exists regarding the potentially harmful effects of new plant-based bioplastics, characterised by a global production of 1.1 million tons that is expected to reach 4.6 million tons by 2028 [17]. Moreover, their rapid degradation may be associated with an enhanced release of NPLs into the environment [34].

A critical health concern related to long-term exposure to NPLs is the possibility of inducing cancer. Carcinogenesis is a multistage process that consists of three consecutive steps: initiation, promotion, and progression. In the first two steps, a normal cell undergoes mutations that enable it to grow autonomously, followed by the abnormal clonal expansion of the initiated cell during the promotion stage. In the last step, neoplastic cells are transformed into an invasive malignant tumour [27]. Regulatory-based assessment of the carcinogenic potential of a compound should be carried out by conducting a 2-year study on rodents, according to the Organisation for Economic Co-operation and Development test guidelines (OECD TG 451 or OECD TG 453). However, these studies are expensive, time-consuming, and raise ethical issues owing to the large number of animals required. Moreover, they provide little mechanistic information regarding the mechanism of action [40]. Therefore, consistent with current efforts to support new methodological approaches to replace animal testing [30], two validated *in vitro* cell transformation assays (CTAs) (OECD guidance documents, GD 214, and GD 231) have been proposed as alternative methods to simulate the first stages of tumourigenesis [44]. Of these, the Bhas 42 CTA (OECD GD 231) [63] consists of two parallel assays that allow distinguishing tumour initiators from tumour promoters, which act by genotoxic and non-genotoxic mechanisms, respectively [39,51]. The basis of the Bhas 42 assay is the scoring of transformed foci; that is, discrete anchorage-independent altered colonies of morphologically altered cells formed on top of the confluent monolayer of cells [63]. Such transformed foci have been shown to be capable of producing tumours *in vivo*, which is considered the gold standard for carcinogenicity evaluation [22]. Furthermore, as Bhas 42 cells contain an activated oncogene, this assay does not require a preliminary treatment with an initiating (genotoxic) substance in the promotion condition [35]. Consequently, the Bhas 42 assay shows a higher sensitivity than that of other CTA assays and has been confirmed as a highly robust and reproducible assay [24]. In fact, this assay has been recommended for inclusion in the OECD integrated approach to the testing and assessment of non-genotoxic carcinogens [43]. Notably, in addition to soluble chemicals, the assay has been successfully applied for testing different types of nanomaterials (see the review by Hayrapetyan and colleagues [40]), which highlight its potential use for evaluating NPL effects.

To date, no standardised studies have directly evaluated the carcinogenic effects of NPLs *in vivo*, although higher rates of cancer incidence have been reported in synthetic textile and fibre manufacturer workers after several years of polypropylene and polyvinyl chloride fibre-related exposure [64]. In addition, the results of recent *in vitro* and *in vivo* studies performed with macro- and nanoscale pristine PS particles suggest that these particles exhibit tumourigenic potential [13,14,23,50,83]. Several plastic particles, mainly comprised of PS, have also been shown to induce reactive oxygen species formation, inflammation, fibrosis, and genotoxicity. These characteristics, together with their ability to accumulate in cells and tissues, also raise concerns about the carcinogenic potential of such plastic particles [27]. However, owing to the diversity of NPL properties and the complex nature of the carcinogenesis process, the existing evidence is insufficient to support the regulatory classification of these particles as carcinogens.

In the present study, we used the validated Bhas 42 assay to assess the cell-transforming potential of two types of secondary NPLs, with the intention of providing data of regulatory relevance to support the carcinogenic risk assessment of these materials and to provide insights regarding the underlaying mechanisms of action. The analysed NPLs included polyethylene terephthalate (PET) particles generated from sanding commercial plastic water bottles, and polylactic acid (PLA) nanoplastics obtained through PLA pellet degradation, as an example of new bio-based biodegradable plastics. In addition, commercially available pristine PS nanoparticles were included to allow comparisons with previous studies. A broad range of concentrations was tested to comply with OECD GD requirements and to ensure the inclusion of potentially realistic exposure concentrations. To the best of our knowledge, this is the first study to assess the carcinogenic potential of secondary NPLs.

2. Materials and methods

2.1. Particles

PS nanoparticles were purchased as a stable dispersion (50 mg/mL) from Spherotech, Inc. (Chicago, IL, USA). PET nanoparticles were obtained from sanding commercial water PET bottles by following a previously published protocol [78]. In brief, the in-house made PET NPLs were sanded using a rotary diamond burr and sieved through a 0.20-mm mesh. Four grams of the sieved particles were added to 40 mL of 50 °C pre-warmed 90 % trifluoroacetic acid with constant stirring for a minimum of 2 h and then kept under constant agitation overnight. The pellet was resuspended in 400 mL of 0.50 % sodium dodecyl sulphate, sonicated, and allowed to settle in 250-mL graduated cylinders for 1 h. The top 100 mL fractions were used to prepare the stock suspensions (5 mg/mL) following an adapted Nanogenotox protocol [46], as previously described [7]. Nanoparticles of PLA were obtained by solvent evaporation, combined with a mini emulsion technique, as described previously [1]. To proceed, a pre-mini emulsion was prepared by adding the aqueous phase consisting of Pluronic® F-127 BioReagent and polyvinyl alcohol (Sigma-Aldrich, Darmstadt, Germany) dissolved in 120 g water (0.25 % and 2 % wt, respectively) to the organic phase composed of 1 g of PLA dissolved in 30 g dichloromethane and stirring magnetically for 60 min. Ultrasonication under ice-cooling was applied for 120 s at 80 % amplitude, using a Bandelin Electronic UW2200 sonicator (Berlin, Germany). The obtained mini emulsion was transferred to a round bottom flask to evaporate the organic solvent under pressure, resulting in a final stock suspension of 20 mg/mL. The concentration of nanoparticles in the PET and PLA stock suspensions was calculated as the solid content, by weighing dried samples.

The fluorescence-labelled version of these plastic particles was also used in this study. Fluorescent PS (yellow) with comparable characteristics to those of the non-labelled PS, was purchased from Spherotech, Inc. Alternatively, PET and PLA particles were labelled with iDye Poly Pink (Rupert, Gibbon & Spider, Inc., Healdsburg, CA, USA). Briefly,

0.01 g of the dye was mixed with 1 mL of the stock particle suspension and incubated at 70 °C for 2 h. After cooling, the suspension was added to 9 mL Milli-Q water in an Amicon Ultra-15 Centrifugal Filter Unit (Merck, Darmstadt, Germany) and centrifuged at 4000 rpm for 15 min. This washing step was repeated twice, after which the particles were collected and suspended in a final volume of 1 mL Milli-Q water.

2.2. Particle characterisation

For characterisation means, PS, PET, and PLA particle suspensions were prepared at a final concentration of 50 or 100 μg/mL in low conductivity Milli-Q (Ultrapure Type 1, 18.2 mScm-1) water and in high conductivity Dulbecco's modified Eagle medium, nutrient mixture F-12 (DMEM/F-12) purchased from Gibco® Life Technologies (Carlsbad, CA, USA).

2.2.1. Transmission electron microscopy

Electron microscopy was carried out using a JEM 1400 transmission electron microscope (JEOL Ltd., Tokyo, Japan). The microscope was operated at 120 kV and images were obtained using a Gatan ES1000 W Erlangshen CCD camera (AMETEK, Inc., Devon-Berwyn, PA, USA). Three different carbon support films covering 400 square mesh copper grids at micro- to nano-scale were dipped three times in the corresponding particle suspension (prepared at a concentration of 50 μg/mL in medium), labelled, and left to dry on a Petri dish overnight prior to evaluation. Particle sizing was performed by measuring the Martin diameter of a minimum of 150 particles from random fields using the Fiji extension of ImageJ version 265 1.8.0_322 (National Institutes of Health, Bethesda, MD, USA). Data were processed using GraphPad Prism 9.3.1 software (GraphPad, La Jolla, CA, USA).

2.2.2. Dynamic light scattering analyses

To investigate the particle behaviour in suspension, two different strategies were applied for both high and low conductivity media and for the three investigated NPLs, following a previously published procedure [7]. Briefly, particle size was determined using dynamic light scattering (DLS) and multiangle dynamic light scattering (MADLS) by placing 1 mL of nanoparticle suspension on a DTS0012 cuvette. Additionally, 1 mL of the particle suspension was transferred to a DTS1070 cuvette to determine the Z-potential and DLS. All measurements were carried out in triplicate on a Zetasizer® Ultra red label analyser, and the data were analysed using ZS-xplorer software 1.1.0.656 (both from Malvern Panalytical Ltd., Cambridge, United Kingdom). Data were processed using GraphPad Prism 9.3.1 software.

2.2.3. Nanoparticle tracking analysis

Particle size (nm) and surface area concentration (nm^2/mL) were determined using a combination of light scattering and Brownian movement with a Nanosight NS300 system from Malvern Panalytical Ltd. (Cambridge, United Kingdom). Working solutions (100 μg/mL) were vigorously vortexed and diluted (1:50) in Milli-Q water in a pressured air pre-cleaned 20 mL glass vial. The vial was then agitated at 1000 rpm using an SA8 vortex (Merck KGaA). One mL was carefully injected into the Nanosight microfluidic system using a syringe. The collection speed was decreased from 1000 to 50 a.u. and independent measurements were carried out. Data were acquired using a 488-nm laser and an sCMOS detector. All measurements were performed triplicate. Data were processed using GraphPad Prism 9.3.1 software.

2.2.4. Fourier-transform infrared spectroscopy (FTIR)

Chemical identity of the functional groups of the three different nano polymer suspensions was evaluated using a Hyperion 2000 system (Bruker Corp., Billerica, MA, USA). Samples were prepared by pipetting 10 μL of the aqueous suspension (10 mg/mL) of each NPL on a folding mirror and left to dry for one week prior to evaluation, which was performed using a Vertex 80 device (Bruker Corp.). The peaks corresponding to the polymer of interest were identified by analysing the interferograms. All measurements were carried out in triplicate. Data were processed using GraphPad Prism 9.3.1 software.

2.3. Bhas 42 establishment and cell culture

Bhas 42 cells were purchased from the Japanese Collection of Research Bioresources (JCRB) Cell Bank (Osaka, Japan) at passage 15. Cells were then expanded as recommended by the OECD guidance [63] to generate a cell stock by culturing them in M10F medium at 37 °C and 5 % CO_2. This medium consisted of minimum essential medium (MEM; ThermoFisher, Whaltham, MA, USA) supplemented with 1 % penicillin-streptomycin (ThermoFisher), 1 % L-glutamine (VWR, Radnor, PA, USA), and 10 % foetal bovine serum (FBS; ThermoFisher). After reaching 70 % confluence, cells were subcultured with 0.25 % trypsin (Biowest, Nuaillé, France). At passage 18, 500,000 cells per vial were frozen using 95 % cold M10F and 5 % dimethyl sulfoxide (DMSO; Merck). All CTAs were performed using this batch of cells, confirmed to be mycoplasma-free. DF5F medium was used to perform all CTAs. This medium consisted of DMEM/F-12, 1 % penicillin-streptomycin, and 5 % FBS. All the assays were performed using a pre-screened FBS batch to avoid the spontaneous formation of foci.

2.4. Bhas 42 treatments

PS, PLA, and PET stock suspensions (50, 20, and 5 mg/mL, respectively) were diluted in distilled water, and the corresponding working suspensions were added to DF5F medium at 1 % (for PS and PLA), or at 4 % (for PET) to reach the desired final concentrations of 6.25, 12.5, 25, 50, 100, and 200 μg/mL. The concentration of the plastic particles was selected according to an independent cell growth assay. As positive controls, 3-methylcholanthrene (MCA, Sigma-Aldrich) and 12-O-tetradecanoylphorbol 13-acetate (TPA, Sigma-Aldrich) were diluted in DMSO to attain a 1 mg/mL stock solution. MCA and TPA stock solutions were diluted with DMSO and added to DF5F medium at 0.1 % to reach a final concentration of 1 and 0.05 μg/mL, respectively. Bhas 42 cells were also treated (1 %) with caffeine (Sigma-Aldrich) at 100 μg/mL. This concentration was chosen based on the results of Sakai *et al.* [70]. Specifically, caffeine powder was weighed and diluted in distilled water to reach a stock concentration of 10 mg/mL. Distilled water and DMSO, used as vehicles, were also added to the cells as negative controls. The fluorescent counterparts were used to track particle internalisation. Towards this end, labelled PS, PLA, and PET particles were diluted to reach a final concentration of 200 μg/mL in each well. The negative controls were incubated with DF5F medium.

2.5. Cell transformation assay and concurrent cell growth assay

The cell transformation and concurrent cell growth assays were performed as recommended by the OECD, in accordance with the six-well-format protocol [63]. The CTA includes both the initiation and promotion assays. Briefly, Bhas42 cells (passage 18) were thawed and cultured in M10F medium until reaching 70 % confluence. Cells were then subcultured in DF5F medium; upon reaching 70 % confluence, they were seeded (day 0) into 6-well plates at a density of 4,000 cells/well (for the initiation test) or 14,000 cells/well (for the promotion test). Cells were treated with either PS, PLA, or PET particles (6.25–200 μg/mL) either from day 1 to 4, or from day 4 to 14, for the initiation and promotion assays, respectively. MCA (1 μg/mL) and TPA (0.05 μg/mL) were used as positive controls for the initiation and promotion assays, respectively. Caffeine (100 μg/mL) was used as a chemical negative control in both assays. As described previously, cells were treated with vehicles (distilled water and DMSO) as negative controls. The additions of both positive and negative controls to the cells followed the same schedule as the NPL treatments. Culture medium changes to fresh medium were performed on days 4, 7, 11, and 14 in the initiation assay. In

the promotion assay, medium was exchanged with DF5F containing either NPLs, MCA, TPA, water, DMSO, or caffeine on days 4, 7, and 11, whereas fresh DF5F was added on day 14. On day 21, the medium was removed from all conditions of the initiation and promotion assay, and cells were fixed with absolute ethanol and stained with 5 % Giemsa (Sigma-Aldrich) for at least 30 min. Then, cells were washed with running tap water to remove the excess stain. Foci from six wells were counted for each condition (six replicates per condition) using a Wild M3Z stereomicroscope (Wild Heerbrugg, Gais, Switzerland) with an external Leica Cold Light Source 100 (Wetzlar, Germany) following the criteria established in the OECD guidance.

The concurrent cell growth assay was performed on day 7. Briefly, Bhas 42 cells were seeded specifically for cell growth and exposed to the different conditions, following the same indications as described for the CTA. On day 7, cells were washed, detached using 0.25 % trypsin, and resuspended in DF5F. Live cells were counted using Trypan-Blue and EVE™ Counting Slides (NanoEntek, Seoul, Korea) with an EVE™ Plus Automated Cell Counter (NanoEntek). Three replicates per condition were analysed and the relative cell growth of cells treated with NPLs, MCA, TPA, or caffeine was determined referring to the corresponding vehicle condition (distilled water or DMSO).

2.6. Internalisation assay

To evaluate whether NPLs internalise into Bhas 42 cells, confocal microscopy was used. Bhas 42 cells were seeded into 6-well plates containing sterile 16 mm coverslips. The same cell culture procedures as described for the CTA (Section 2.5; six replicates per condition) were followed. Bhas 42 cells were treated with 200 μg/mL PS, PLA, or PET particles following the same treatment schedule as described for the CTA, both for initiation and promotion assays. At day 7, cells were washed with phosphate-buffered saline (Gibco Life Technologies), and plasma membranes were stained either with CellMask Deep Red or CellMask Green (both from ThermoFisher) (1:1000) for 10 min at 37 °C. Samples were fixed with 4 % formaldehyde and nuclei were stained with 1 μg/mL 4′,6-diamidino-2-phenylindole dihydrochloride (DAPI; Sigma-Aldrich) for 10 min at room temperature. Samples were then mounted by placing the coverslips upside down over a slide, using Eukitt® Quick-hardening mounting medium (Sigma-Aldrich). Imaging was performed using a Zeiss LSM880 confocal microscope (Darmstadt, Germany). The objective used was Plan-Apochromat 40x/1.4 Oil DIC M27 (refractive index 1.518). Images were acquired by taking z stacks of the whole sample thickness. Samples treated with PS were imaged using a 488-nm Argon laser, whereas a 405-nm Diode laser and a 633-nm Helium-Neon laser were used to image DAPI and CellMask Deep Red, respectively. Samples treated with PLA or PET were imaged with a 561-nm Diode laser to detect the NPLs, while a 405-nm Diode laser and a 488-nm Argon laser were used to image DAPI and CellMask Green, respectively. ImageJ software with the Fiji extension was used to process and analyse the images.

2.7. Statistical analyses

GraphPad Prism 9.3.1 software was used for the statistical analyses. Cells treated with NPLs were compared with those treated with the negative control (distilled water) using one-way analysis of variance (ANOVA) with the Dunnett's post-test as recommended by the OECD [63]. In the case of statistical significance, dose dependency was evaluated by linear regression analysis. Cells treated with caffeine were also compared to their vehicle control (distilled water) using the t-test, as well as MCA and TPA conditions, which were compared to the DMSO condition. The effects were considered significant if $p < 0.05$. Data are shown as the mean ± SD.

3. Results

3.1. Particle characterisation

For particle characterisation, graphic representation and analysis were conducted by following the recommended guidelines from the European Commission [29]. TEM images for PS, PLA, and PET NPLs are shown in Fig. 1A, D, and G, respectively. PS and PLA particles exhibited a spherical shape, whereas PET particles lacked a regular shape. In addition, the corresponding size distribution for each particle based on the dry state TEM measurements is shown in Fig. 1B, E, and H. A summary of the average size and polydispersity index (PDI) of each NPL is presented in Table S1 of the Supplementary Material. PS NPLs showed a clearly monodispersed size distribution, which is reflected not only in the narrow peak observed in Fig. 1B but also in the calculated PDI of 0.05 with an average particle size of 70.25 nm and a standard error of the mean (SEM) of 1.28. Similarly, PLA NPLs exhibited a narrow peak with a PDI value of 0.05, with an average size of 211.78 nm and a SEM of 3.64. Alternatively, PET NPLs presented a very broad multimodal peak with a high PDI of 2.94. Whereas the average particle size remained on the nanoscale (90.18 nm), the SEM was comparatively high (12.54), which could be attributed to the fact that approximately 4 % of the PET NPLs were larger than 500 nm.

The chemical identity of the NPL suspensions was confirmed using FTIR analysis, as shown in Fig. 1C, F, I. More detailed analyses of the corresponding infrared spectra are included in Fig. S1 of the Supplementary Material. The obtained interferograms were compared with previous reports of the representative bands present in polymer spectra [33,49,62], and then assigned to the corresponding bands. The PS NPL sample (Fig. 1C and Fig. S1a) showed the characteristic aromatic C–H stretch from 2800 to 3060 cm^{-1} and aliphatic C–H stretch (2800–3000 cm^{-1}). Benzene fingers from 1650 to 2000 cm^{-1} related to the monosubstituted benzene ring of polystyrene could be observed as well as the aromatic C═C stretching close to 1600, 1492, and 1452 cm^{-1}. In the case of PLA NPLs (Fig. 1F and Fig. S1b), the typical stretching frequencies for C═O were visible at 1746 cm^{-1}, whereas asymmetric and symmetric -CH_3 stretching was present in the 2940–3000 cm^{-1} region; C–O stretching was observable close to 1080 cm^{-1}, and characteristic -CH_3 asymmetric and symmetric bending could be seen, respectively, at 1452 and 1361 cm^{-1}. In the case of PET NPLs (Fig. 1I and Fig. S1c), a dominant peak for carboxylic acid C═O stretching is observed at 1730 cm^{-1}, while the other dominant peaks, observable close to 1240 cm^{-1}, have been assigned to the terephthalate group and describe the presence of C═O in plane bending, C-C stretching, and (C═O)–O stretching. On 1050 and 1096 cm^{-1} the methylene vibrations and vibrations of the ester C-O bond are observable.

With regard to hydrodynamic behaviour, the corresponding size distributions in water and medium as measured by DLS are shown in Fig. 2A, D and G for PS, PLA, and PET dispersions, respectively. In addition, Table S2 summarises the average size, PDI, and Z-potential value of each NPL in both dispersants; a full description of DLS, MADLS values, and correlation coefficients for all measurements can be found in the Supplementary Material (Fig. S2). For all three investigated NPLs, no shifts in the average size beyond 10 % were observed when different dispersants were used for resuspension. Pristine PS NPLs showed the most stable particle size distribution, as illustrated by Fig. 2A. Similar size distributions were observed regardless of the dispersant used, even though a considerable shift in the surface potential occurred: from − 27.30 mV in water to − 45.30 mV in medium (Table S2). A similar behaviour in the Z-potential value was observed for PET NPLs, which shifted from − 15.00 mV in the water to − 41.40 mV in medium; however, the smaller size fraction that was easily detected by TEM was largely overlooked by the DLS technique, reiterating the importance of the multitool description of particles with regard to biological applications. The use of DF5F culture medium instead of low conductivity Milli-

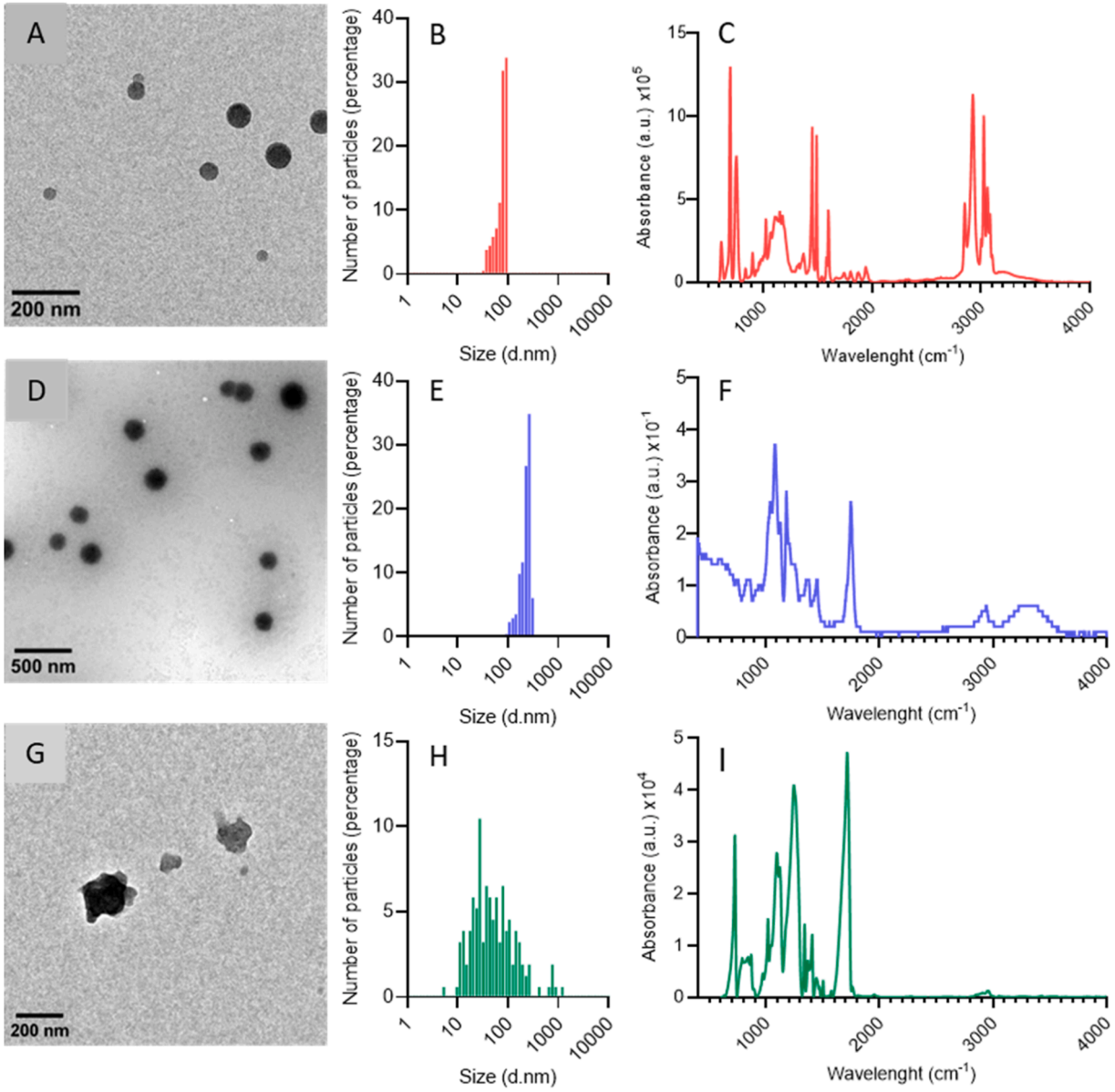

Fig. 1. Characterisation of polystyrene (PS), polylactic acid (PLA) and polyethylene terephthalate (PET) nanoplastics (NPLs) in dry state. Transmission electron microscopy images of PS (A), PLA (D), and PET (G) NPLs dispersed in DF5F medium. Size distribution calculated from the same samples in terms of percentage of particles by Martin diameter (from a minimum of 150 particles) for PS (B), PLA (E), and PET (H) NPLs. Infrared spectra, measured by Fourier-transform infrared spectroscopy (N = 3), of PS (C), PLA (F), and PET (I) NPLs dispersed in Milli-Q water (a.u., absorbance units).

Q water revealed part of the smallest fraction of PET NPLs observable in Fig. 2G. This apparently contradictory result may indicate the intrinsic inconvenience of DLS when multimodal highly polydispersed samples are measured, but it is also a crucial factor to consider when more relevant true-to-life materials are used. Moreover, it is important not to misconstrue the results and contrast it with those obtained using different techniques. In contrast, the Z-potential behaviour of PLA NPLs was opposite to that observed with the other nano polymers, shifting through the less negative values (from −21.00 mV to −1.60 mV) when the dispersant composition was more conductive (Table S2). This behaviour can also be observed in Fig. 2D, where some particle agglomeration can be clearly observed on the dashed lines representing the size distribution. However, for water-dispersed particles, the bigger peak is highly consistent with the dry state TEM values (Fig. 1E), although DLS revealed some important aggregation at the 700 nm region, which was reflected in the average values.

The hydrodynamic behaviour of the NPLs was also investigated by nanoparticle tracking analysis (Fig. 2B, E, and H), which is assumed to be a more reliable method than DLS for polydispersed suspensions [16]. The average sizes were 81.70 ± 0.30, 172 ± 1.10, and 205.60 ± 7.7 nm for PS, PLA, and PET nanoparticles suspended in water. These values were lower than those obtained by DLS for PLA and PET, and similar for PS NPLs, which showed the smallest hydrodynamic size by both methods. In comparison, when considering the surface area concentration (Fig. 2C, F, and I), PS sample also showed the highest percentage of particles with the greatest surface area concentrations together with the narrowest distribution of values, compared to those of the other two NPLs. The distribution of surface area concentration of PET NPLs revealed the multimodal and therefore the environmentally representative nature of these in-house generated particles.

3.2. *Cell-transforming capacity of the nanoplastics*

Before beginning the CTA, a cell growth assay including NPL

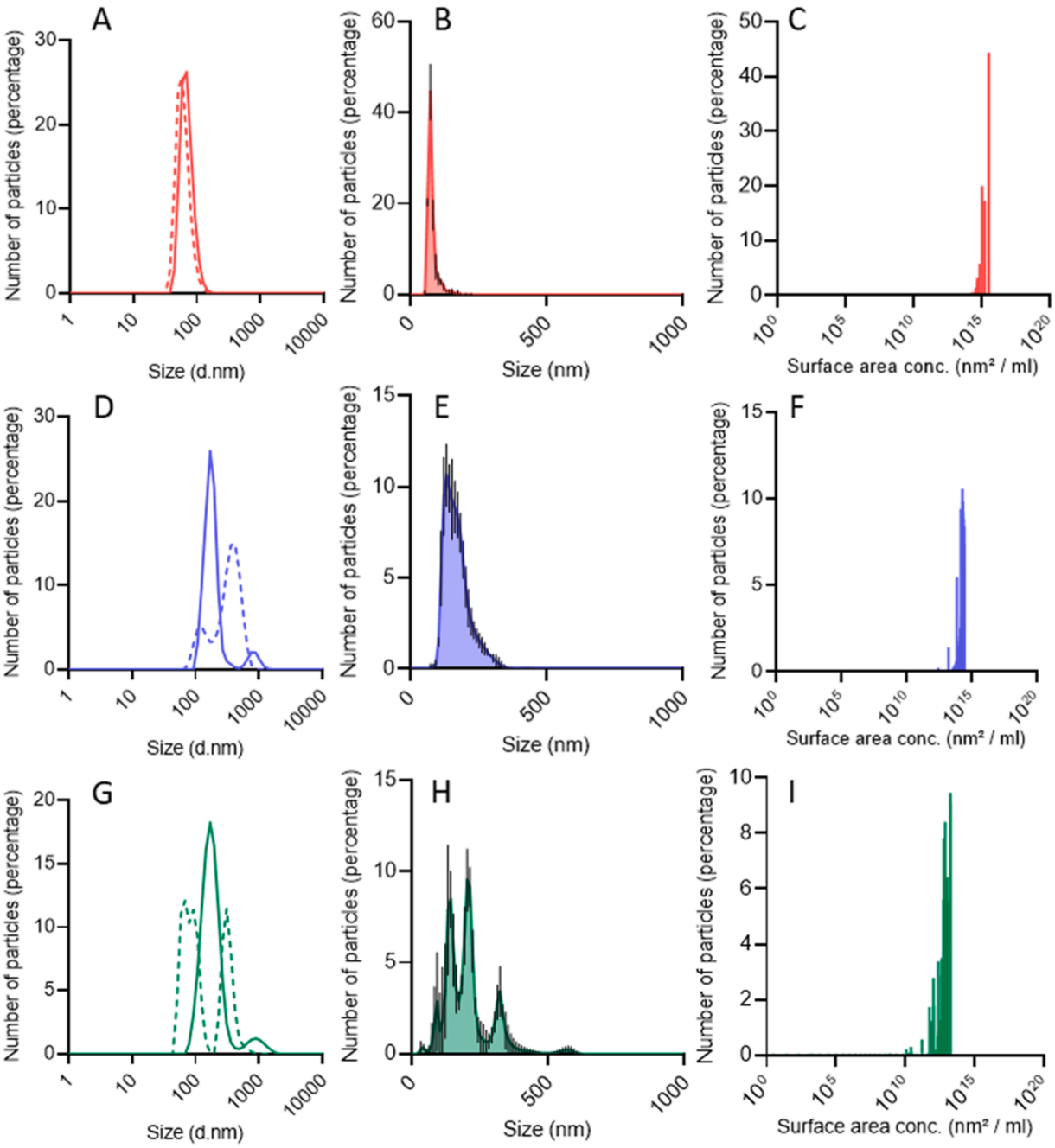

Fig. 2. Characterisation of polystyrene (PS), polylactic acid (PLA) and polyethylene terephthalate (PET) nanoplastics (NPLs) in dispersion. Hydrodynamic size distribution measured by dynamic light scattering (N = 3 replicates) of PS (A), PLA (D). and PET (G) NPLs dispersed in Milli-Q water (solid lines) and in DF5F medium (dashed lines). Hydrodynamic size distribution (B, E, and H) and distribution of the surface area concentration (C, F, and I) measured by Nanotracking analyses (N = 3 replicates) of PS (B and C, respectively), PLA (E and F, respectively) and PET (H and I, respectively) NPLs dispersed in Milli-Q water.

concentrations ranging from 6.25 to 200 μg/mL was conducted to select the concentrations to be used in the initiation and promotion assays. As none of the concentrations showed a toxic response compared to that of the untreated cell cultures (data not shown), the highest concentration to be tested was set to 200 μg/mL, as previously recommended for nanomaterials [73]. In addition, the lower concentrations were chosen according to the application in previous studies, in which treatments ranged from 1 μg/mL [45] to 250 μg/mL [47] of plastic materials.

The results of the CTA are shown in Fig. 3. In agreement with the preliminary cell growth assay, none of the NPLs induced a decrease in Bhas 42 cell proliferation. In contrast, PS appeared to enhance the cell growth in the initiation assay, whereas PET increased Bhas 42 cell growth in both the initiation and promotion assays. With regard to the cell-transforming capacity of the materials, the positive controls MCA and TPA induced a significant increase in the number of transformed foci in the initiation and promotion assays, respectively. In comparison, caffeine, which was used as a negative control in both assays, showed a similar number of transformed foci as resulting from the water-treated cultures, except for the promotion assay with PET NPLs where the number of caffeine-induced foci was significantly lower than that of the vehicle (Fig. 3F). In the initiation assay, none of the NPLs showed an increase in the number of transformed foci compared to those with the negative control (Fig. 3A, C, and E). Similar results were obtained with PS and PLA in the promotion assay, where neither NPLs showed any

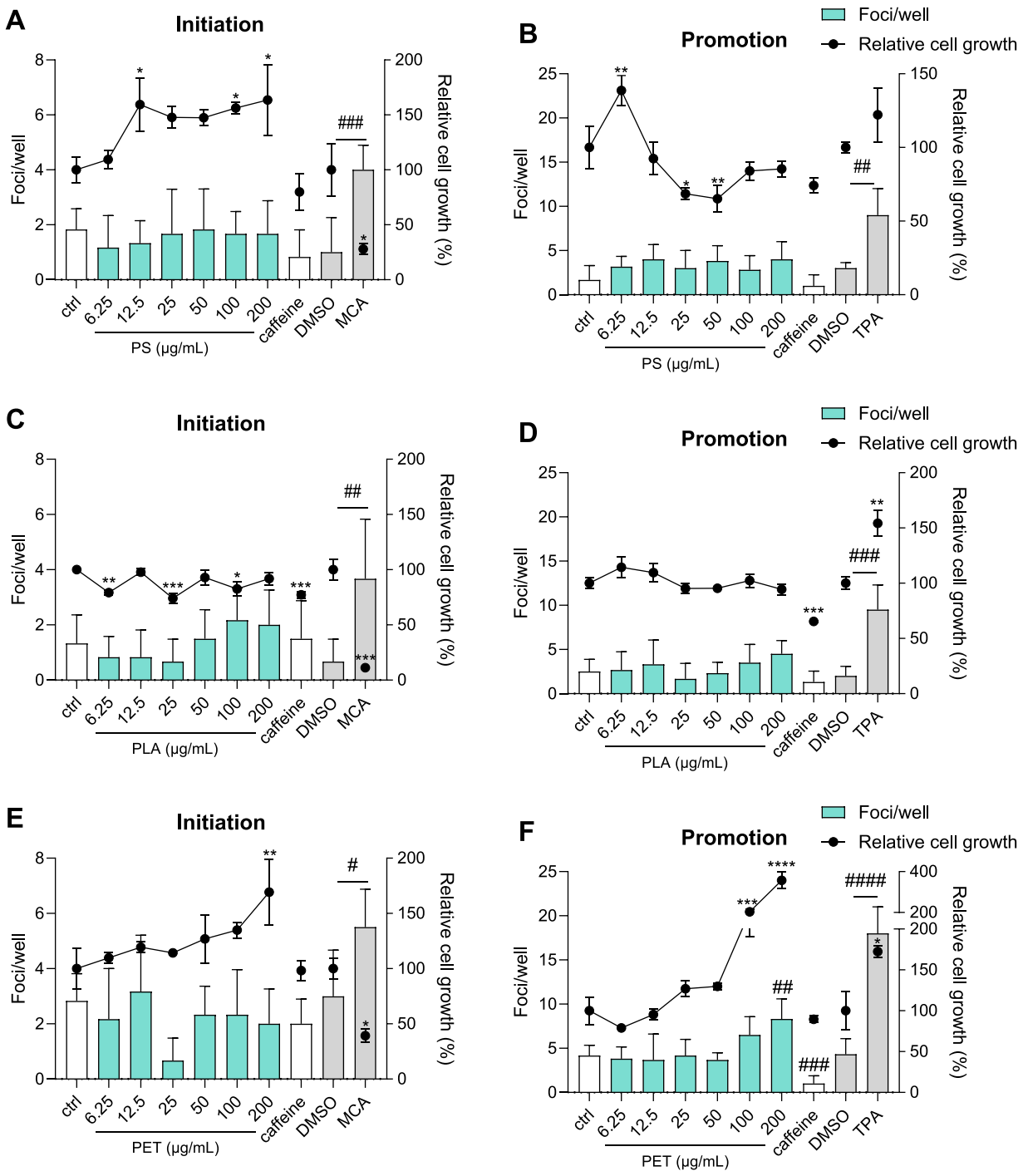

Fig. 3. Number of transformed foci per well (bars; N = 6 replicates) and percentage of relative cell growth referred to the corresponding vehicle (dots and lines; N = 3 replicates), induced by polystyrene (PS; A and B), polylactic acid (PLA; C and D), and polyethylene terephthalate (PET; E and F) nanoplastics (NPLs) in the Bhas 42 cells initiation and promotion assays. 3-methylcholanthrene (MCA), and 12-O-tetradecanoylphorbol 13-acetate (TPA), which are the positive controls for the initiation and promotion assays, respectively, were compared with their solvent DMSO. Caffeine (negative control) and PS, PET, and PLA NPLs were compared to the control condition (H_2O, used as a vehicle). Asterisks indicate statistical significance relative to cell growth at *p < 0.05, **p < 0.01, ***p < 0.001 and ****p < 0.0001. Hash marks indicate statistical significance relative to the number of foci/well at #p < 0.05, ##p < 0.01, ###p < 0.001 and ####p < 0.0001. PET NPLs also induced a statistically significant dose-response (p < 0.0001) in the promotion assay (F).

transforming activity (Fig. 3B and D). Conversely, PET treatment significantly increased the number of transformed foci among Bhas 42 cells in the promotion assay, and also showed a significant dose-dependent response (Fig. 3F). The dispersion solution of nano-PET (0.05 % BSA-based solution), tested in parallel experiments, induced no effect (data not shown).

3.3. Internalisation of nanoplastics into Bhas 42 cells

The internalisation of NPLs into Bhas 42 cells was assessed using confocal microscopy after cells were exposed to the NPLs, following the treatment schedule described for the initiation and promotion assays (Section 3.2) up to day 7, when samples were fixed and stained for subsequent analysis. PS, PLA, and PET particles were able to internalise

into Bhas 42 cells. As shown in Fig. 4, PS, PLA, and PET particles were observed in the cell cytoplasm and near the nucleus upon reproduction of the initiation assay conditions. PET NPLs showed a higher accumulation rate than that of the other two NPLs with this treatment schedule (Fig. 4E). PS, PLA, and PET particles were also found inside the cell membrane following the promotion condition (Fig. 5), with PS and PET NPLs localising closer to the cell nuclei (Fig. 5C and E). The internalisation rate for PET NPLs was slightly higher than that for the other NPLs in these conditions, although not as pronounced as with the initiation schedule. In contrast, no NPL signals were detected in the untreated conditions either for the initiation (Fig. 4A and B) or promotion assay (Fig. 5A and B).

4. Discussion

In the present study, the cell transforming capacity of three different NPLs was assessed by using a validated *in vitro* CTA [70], whose suitability for testing particulate materials has been previously confirmed [35]. Among the tested NPLs, only PET NPLs— which are predominantly present among environmental secondary NPLs [54] —demonstrated

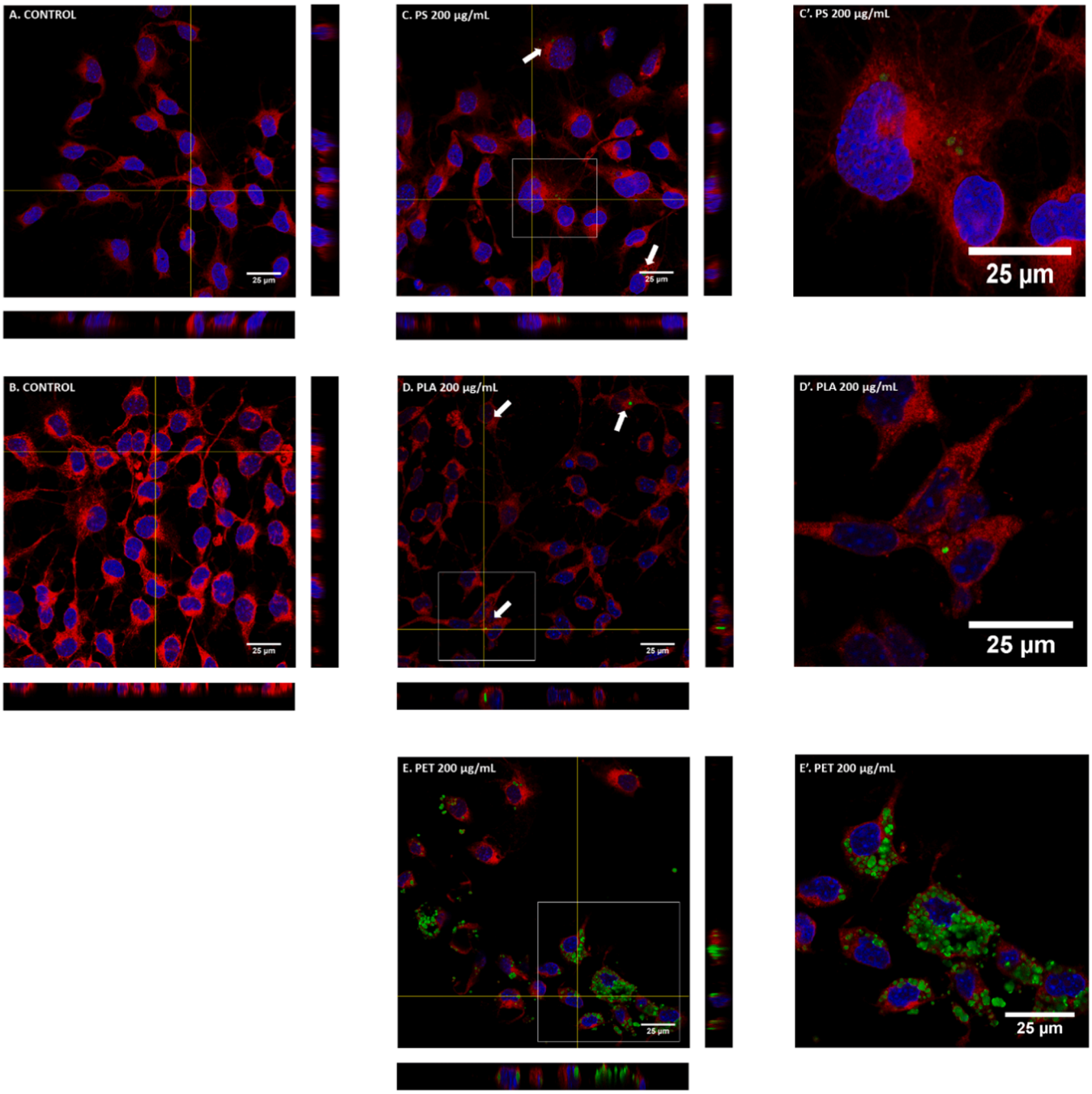

Fig. 4. Internalisation of polystyrene (PS), polylactic acid (PLA), and polyethylene terephthalate (PET) particles into Bhas 42 cells after 4 days of exposure (from day 1 to 4) following the treatment schedule described for the initiation assay until day 7 (N = 6 replicates). Cell membranes are shown in red; cell nuclei are shown in blue; and plastic particles are shown in green. Control samples (A and B) were stained using CellMask Deep Red and CellMask Green, respectively, and DAPI. Cells treated with PS (C and C′) were stained using CellMask Deep Red and DAPI, while cells treated with PLA or PET (D, D′, E, and E′) were stained using CellMask Green and DAPI. Orthogonal views projected from the yellow lines are shown (A-E). White squares (C-E) indicate the zoomed area (C′-E′). White arrows point out some of the particles.

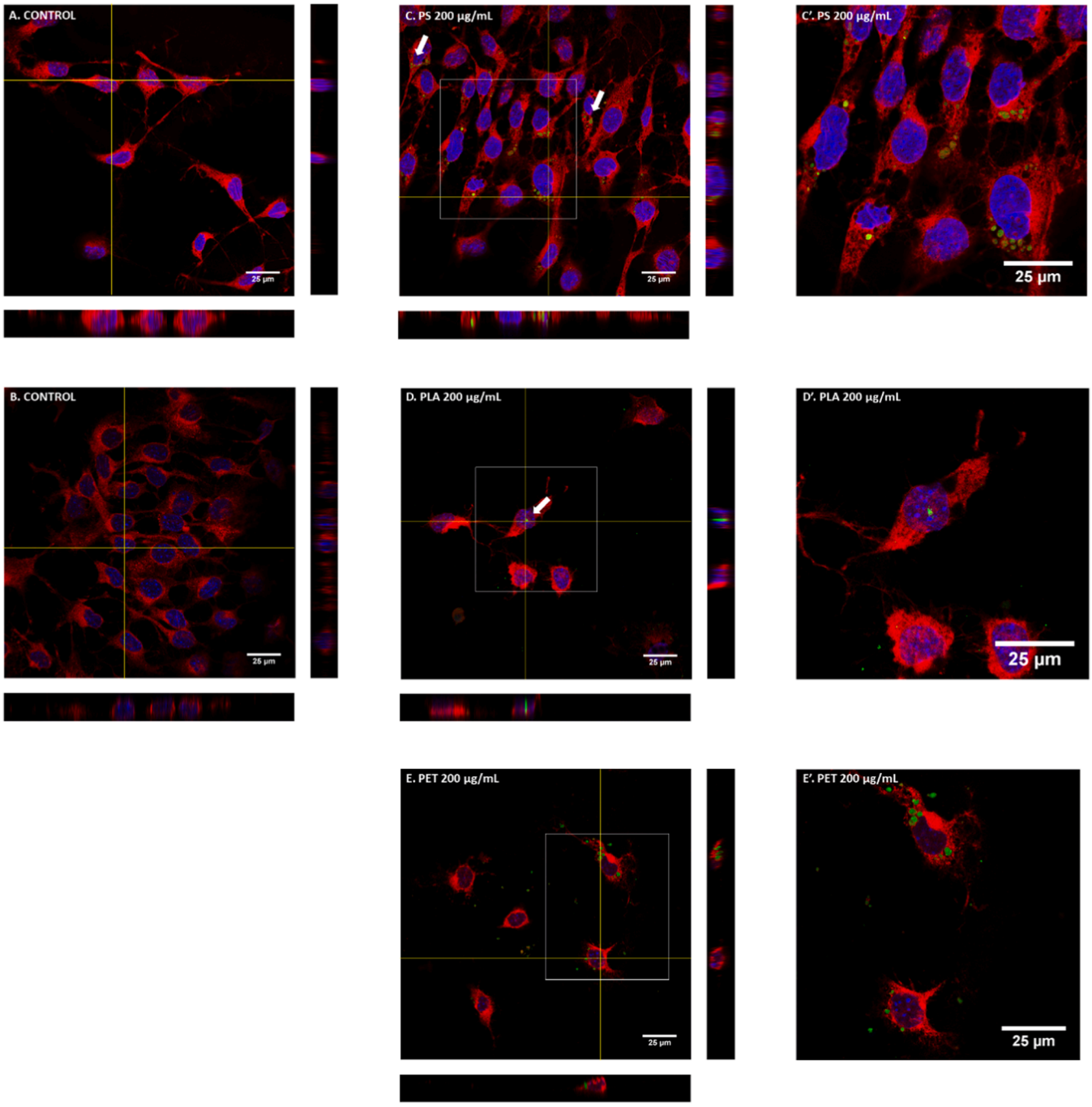

Fig. 5. Internalisation of polystyrene (PS), polylactic acid (PLA), and polyethylene terephthalate (PET) particles into Bhas 42 cells after 3 days of exposure (from day 4 to 7) following the treatment schedule described for the promotion assay until day 7 (N = 6 replicates). Cell membranes are shown in red; cell nuclei are shown in blue; and NPLs particles are shown in green. Control samples (A and B) were stained using CellMask Deep Red and CellMask Green, respectively, and DAPI. Cells treated with PS (C and C′) were stained using CellMask Deep Red and DAPI, while cells treated with PLA or PET (D, D′, E, and E′) were stained using CellMask Green and DAPI. Orthogonal views projected from the yellow lines are shown (A-E). White squares (C-E) indicate the zoomed area (C′-E′). White arrows point out some of the particles.

cell-transforming effects through a tumour promotion mode of action. Although a statistically significant transforming response was only observed at the highest concentration (200 µg/mL), the response was dose dependent. In contrast to the initiating events, which are assumed to be driven by genotoxic mechanisms with a non-threshold mode of action, promoting agents are considered to act by non-genotoxic mechanisms, which show a threshold response [43]. Hence, the highest dose of PET NPLs, corresponding to the lowest observed adverse effect level (LOAEL), can be considered as the *in vitro* threshold value. However, it is not clear whether the corresponding *in vivo* dose could be reached inside human tissues. To date, no reliable data on human exposure exist because the current limitations of the characterisation methods hinder reliable estimations of environmental concentrations of micro- and NPLs [32] as well as their concentrations in tissues and organs [66]. Estimations of human plastic exposure vary from 16 µg of particles being released from a single cup of tea [41] to an average total weekly intake of 0.01 to 5 g for an average 70-kg person [25,5,71,82]. Alternatively, an average concentration of 1.6 µg/mL of different types

of plastic polymers larger than 700 nm was reported in blood samples from healthy donors [55]. However, most of the micro- and NPLs are not expected to remain in the bloodstream but to translocate and accumulate in different organs [76].

Although PET NPLs alone showed a significant promoting capacity only at the highest concentration tested, humans are usually co-exposed to NPLs and other contaminants in real-life situations [67,85], which may also induce initiating or promoting activities. For example, several heavy metals (*e.g.*, chromium) are well-known genotoxic carcinogens [42]. In comparison, both initiating and promoting modes of action have been shown by different types of polycyclic aromatic hydrocarbons [9]. Therefore, co-exposure of humans to a mixture of PET NPLs and other environmental pollutants may result in an increased risk of cancer development compared to that afforded by the exposure to PET materials alone. In particular, the same PS NPLs as used in the present study increased a set of cancer hallmarks, such as the acquisition of invasion and migration abilities together with a higher capacity of anchorage-independent grow and colony formation, when a pre-transformed cell model of mouse embryonic fibroblasts (MEFs) was co-exposed for 12 weeks to relatively low concentrations of PS NPLs (25 μg/mL) and a human carcinogen arsenic (2 μM As^{III}) compound. However, such effects were not observed when the cells were only treated with the same concentration of PS NPLs alone [14], although a longer exposure time (24 weeks) yielded an alteration of early tumoural biomarkers [13]. Hence, the combination of NPLs and other pollutants may have synergistic effects and produce significant toxic effects at concentrations below their individual LOAELs, as has been reported for chemical mixtures [52]. Nevertheless, antagonist effects between plastic particles and pollutants have also been reported [19]. Therefore, it is not yet possible to predict the real-life effects of the co-exposure of PET or other NPLs with different environmental pollutants, and further research is needed to better understand combined exposures to multiple pollutants.

Unlike PET NPLs, neither of the other NPLs tested in the present study (PS and PLA) showed cell-transforming effects in the Bhas 42 assay. The different behaviour of the materials might be due to their different chemical composition. The protein composition of the corona that is formed on the surface of particles, which is predominantly driven by the nature of the polymer particles, could influence particle uptake [45]. As shown in the internalisation experiments, PET NPLs appeared to internalise into the Bhas 42 cells more efficiently than the other two NPLs, which may result in the actual exposure of a higher proportion of cells. These results agree with those of Deng *et al.* [26], who found a much higher uptake of nano-PET particles (191.6 ± 0.9 nm) than that of nanoscale low density polyethylene (160.5 ± 1.9 nm) particles after incubating murine macrophage RAW264.7 cells for 24 h with 4 μg/mL of plastics. Nevertheless, nano-PET particles were also more efficiently internalised than micro-PET (1.85 ± 1.02 μm) particles [26], indicating that the cellular uptake was size-dependent. A similar pattern was observed in BALB/3T3 mouse cells (from which Bhas 42 cells were developed) treated with nano-sized and bulk forms of titania particles [77]. However, in the present study, PET NPLs showed higher average hydrodynamic size than that of the other NPLs (Fig. 2). Hence, size alone cannot explain the observed behaviour. Moreover, the dispersibility of the NPLs may have influenced both internalisation and cell-transforming potential, as PET NPLs showed a predominantly polydispersed particle size distribution compared to those shown by PS and PLA NPLs (Fig. 2 and Table S2). The combination of micro- and nanoscale PS particles yielded a higher toxicity in mice than that from the application of homogeneous particle sizes [57]. In addition, PET NPLs also differ from PS and PLA NPLs with regard to other particle properties, such as shape, surface charge, or weathering process, which are also known to affect the internalisation mechanisms of particles and, hence, their toxicological profile [47,80]. This observation highlights the relevance of carrying out a thorough characterisation of the NPLs as well as cellular internalisation studies when evaluating their potentially hazardous effects.

Cell growth enhancement was induced by PET and PS particles, although only in the initiation assay for the latter, which may be a consequence of the tumour transforming capacity of the NPLs. In fact, increased cell proliferation is considered an early cell transformation biomarker [15,75]. However, the PS- and PET-induced enhancements in the initiation assay (Fig. 3A and E, respectively) were of lower magnitude (maximum values of 163 % and 169 %, respectively) than that induced by PET in the promotion assay (Fig. 3F), which was especially exacerbated at the two highest concentrations (203 % and 357 % at 100 and 200 μg/mL, respectively); these also showed an increased number of foci per well compared to the number in the negative control (although statistical significance was only attained at the highest concentration). The growth of transformed cells may have been promoted by the required restriction of serum to 5 % in the culture medium when performing the assays, as tumour cells become progressively independent of certain cell nutrients [24]. However, PS NPLs did not show any additional cell transforming potential in the present study. These results disagree with those of Kim *et al.* [50], who investigated the tumourigenesis capacity of micro-sized PS (PS MPLs, 9.5–11.5 μm) in BALB/c nude mice subcutaneously injected with gastric cancer NCI-N87 cells that had been previously exposed for 4 weeks to 8.61×10^5 PS MPLs/mL. Accelerated tumour growth was observed in those animals compared to that in the control group, which consisted of animal injected with untreated cells. In addition, BALB/c nude mice administered with 1.72×10^4 particles/mL of the same PS MPLs daily for 4 weeks by oral gavage exhibited differential expression of 194 genes related to digestive system disease and cancer, and reduced survival rate. In a recent study, *in vivo* exposure for 27 days to PS NPLs (100 nm; 10 mg/L) *via* drinking water significantly accelerated the growth of tumours in BALB/c nude mice that were induced by subcutaneous injection of epithelial ovarian cancer HEY cells [23]. Gene expression analyses revealed that immune-related responses and the tumour microenvironment pathway were significantly enriched. In comparison, a significantly disturbed tumour growth microenvironment favoring *in situ* colorectal tumour growth had previously been described in the colon of BALB/c mice continuously administered with PS or polyethylene NPLs (approximately 500 nm for both; 10 mg/kg/day) for one week and, subsequently inoculated with murine colorectal carcinoma CT26-Luc cells near the colon [83]. Furthermore, induction of fibrosis, a hallmark of cancer [21] has been described in a couple of studies with Wistar rats that were administered 5 and 50 mg/L of PS MPLs (0.5 μm) daily for 90 days in drinking water [6,58]. Fibrosis-related factors were also significantly increased in the lung of ICR mice exposed to 4 to 16 μg/mL of PS MPLs (0.5 μm) by inhalation for 2 weeks [48]. Massive collagen deposition was also observed in the liver tissue of high-fat diet-fed C57BL/6 mice administered with 10 μg/mL PS NPLs (41.54 nm) every 3 days for 15 days through tail vein injection [56]. Moreover, PS NPLs also exacerbated the oncogenic phenotype of pre-transformed MEFs in long-term *in vitro* studies [13,14]. In addition, the rates of proliferation and migration were increased in different human gastric cancer cells following exposure to 8.61×10^5 particles/mL of PS MPLs (9.5–11.5 μm) for 4 weeks, together with upregulation of CD44, a marker of gastric cancer stem cells [50]. The effects of PS MPLs (2 μm; 20 μg/mL) and NPLs (0.5 μm; 5 μg/mL) were also assessed by metabolomics analyses of normal human intestinal CCD-18Co cells exposed for 48 h, or up to 28 days (either continuously or on alternate weeks) [18]. Acute and chronic exposure caused metabolic rewiring and oxidative stress, with the rearrangement of normal metabolic pathways being similar to that induced by the well-known carcinogen azoxymethane and also observed in HCT15 colon cancer cells [18]. Furthermore, PS NPLs (25–100 nm) increased the expression of several pro-inflammatory cytokines in human gastric adenocarcinoma epithelial (AGS) cells [36] and human lung epithelial A549 cells [72,81]. Notably, 44 nm PS NPLs also induced a slight increase in the expression of the *c*-Myc oncogene in AGS cells [36], which is activated

by numerous oncogenic pathways and, in turn, stimulates many of the metabolic changes that result in malignant transformation [59]. In comparison, the exposure of A549 cells to 25 and 70 nm PS NPLs induced the upregulation of genes involved in cell proliferation, such as *cyclin D* and *E*, and *Ki67* [81]. Cyclins regulate the catalytic activities of cyclin-dependent kinases, whose dysregulation results in uncontrolled cancer cell proliferation [38].

Together, the results of these studies appear to suggest that PS particles may have tumourigenesis capacity. However, such effect was not observed in the present study. Notably, Bhas 42 cells, although initially considered to be derived from BALB /c mice, the same mouse strain used in the above *in vivo* experiments, actually originated from the Swiss mouse. Hence, strain-specific differences may exist regarding sensitivity to the transformation induced by PS particles [24]. Similarly, different cell lines can differ in their sensitivity to transformation [22]. Even for cell models where *in vitro* oncotransformation is sustained by similar gene pathways, the same key signalling pathways may become active at different times [24]. In fact, the transformation response of Bhas 42 cells represents a late stage of the transformation process, whereas those of uninitiated immortalised cells and primary cells represent earlier stages [63]. In addition, as described above, differences in the characteristics of the particles can also affect the way they interact with cells and the resultant toxic effects.

In contrast to PS, few studies have evaluated the adverse effects of other types of plastic particles, especially secondary ones [27,61]. The same true-to-life PET NPLs used in the present study did not increase the levels of DNA damage in THP-1 cells treated for 3 h up to 50 μg/mL [78]. However, increased levels of intracellular reactive oxygen species, loss of mitochondrial membrane potential, and altered protein expression of the autophagy pathway were observed in human primary nasal epithelial cells after a 24-h treatment with 100 μg/mL PET NPLs [7]. In particular, autophagy maintains normal cellular homoeostasis and, when disturbed, may result in tumour initiation and tumour growth processes [60]. Furthermore, PET NPLs also induced high levels of both oxidative stress and DNA damage in exposed *Drosophila melanogaster* [2]. Similar effects were observed when the flies were exposed to titanium-doped PET NPLs (112 nm, approximately 3 % TiO_2 nanoparticles), obtained by grinding opaque PET milk bottles [3]. Notably, low concentrations (up to 7 μg/mL for 3 h) of another type of true-to-life PET NPLs obtained from ground food containers (252 and 107 nm) were able to induce DNA damage in Caco-2 and HepG2 epithelial-like cells [68]. The same particles also induced DNA damage in A549 epithelial cancer cells exposed to up to 125 μg/mL particles for 24 h [4]. In addition, murine macrophage RAW264.7 cells treated for 3 h with 4 μg/mL of nanoscale (191.6 ± 0.9 nm) and microscale (1.83 ± 1.01 μm) PET obtained by cutting and heat-treating food packaging products, showed a suppression of lysosomal activity [26].

PLA NPLs were included in this study as an example of biodegradable materials that may provide solutions to the environmental pollution caused by the petroleum-based polymers. As with other bioplastics, very little information about their potential health hazards exists. No significant cytotoxic effects were observed after the 48 h exposure of monocultures of Caco-2 and HT29 epithelial-like tumour cells to 100 μg/mL of PLA NPLs (~160 nm) extracted from commercially available teabags, although a similar treatment induced a slight barrier disruption in the *in vitro* intestinal Caco-2/HT29 model [11]. Alternatively, exposure of *Drosophila* larvae to the same PLA NPLs used in the present study (up to 1 mg/g food) generated high levels of oxidative stress and DNA damage [1]. Using a mouse model, Wang *et al.* [79] showed that PLA nanoparticles and oligomers, generated by enzymatic hydrolysis of PLA microplastics (25-μm diameter, administered at 1 mg/day for 1 week) during digestion, could permeate the gastrointestinal tract and reach other tissues, accumulating in the intestine, liver, and brain. They also observed severe inflammation in the intestine and colon of the exposed mice, which may have been induced by the inactivation of key immune modulator MMP12. Among the three materials tested in the present study, PLA NPLs induced neither cell transformation in either of the two assays (initiation and promotion), nor marked variation in cell growth compared to that in the negative control, suggesting that for the mechanisms involved in the cell-transforming process detected by the Bhas 42 assay, PLA NPLs do not appear to be hazardous and may be a safer alternative to other plastic materials, such as PET. However, direct comparison among these materials is challenging, as they differ widely in other features (*e.g.*, size, surface characteristics) in addition to chemical composition. For example, a study performed with different micro-sized plastics (including PS and PLA) of similar size (1–4 μm) in mouse macrophage cell lines did not observe acute cytotoxic effects for any of the tested particles, whereas a substantial increase in the levels of reactive oxygen species was induced by PLA and another bio-based particle [45].

In comparison, genotoxic carcinogens act as initiators in the Bhas 42 model. The same PS NPLs as the ones included in the present study were also able to induce DNA damage in Raji-B and TK6 lymphoblastoid cells [69], in blood monocytes and polymorphonucleated cells [10], and in pre-transformed mouse embryonic cells [14]. In these and the above-reported studies, genotoxicity was assessed using the comet assay, which can detect DNA strand breaks and alkali labile sites [61]. In addition, when the assay is complemented with use of the FPG DNA repair enzyme, the induction of DNA oxidative damage can be identified. The obtained results showed that DNA damage can be induced by oxidative and non-oxidative mechanisms. In fact, oxidative stress is assumed to be the main mechanism involved in micro- and NPLs-related toxicity [65] and, together with increased inflammatory responses and induction of mutations, has been described a key event in the developmental pathways of several human cancers [8]. However, the type of DNA damage detected by the comet assay does not necessarily result in mutations, as the damage can still be repaired or the damaged cell can be eliminated [20], which is consistent with the lack of transformed foci observed in the initiation assays for the three materials. Conversely, increased levels of chromosomal mutations, assessed using the cytokinesis-blocked micronucleus assay, have been reported with different types of PS NPLs in human skin Hs27 fibroblasts, colorectal adenocarcinoma cells, human lymphocytes, and lung epithelial A549 cells [61]. These studies further illustrate the principle that, in addition to chemical composition, some nano-specific features (*e.g.*, size, shape, or surface chemistry) can drive the interaction of the materials with the cells and may affect the differential transforming capacity of NPLs, as has been reported for engineered nanomaterials [40]. For example, the *in vitro* cell-transforming potential was triggered by fibrous shape in the case of nanosilver [37], and modulated by surface properties in the case of synthetic amorphous nano-silica [35].

Although the *in vitro* oncotransformation detected by the Bhas 42 model closely correlates with *in vivo* tumourigenicity [63], general agreement holds that no single *in vitro* CTA model can capture the complexity of the multistage carcinogenicity process [15,24]. In fact, recent results from transcriptomic studies pointed out that the Bhas 42 assay appears to be a suitable model for studying the later steps in cancer progression, which mark the progression from preneoplastic to neoplastic lesions in humans [24]. An additional limitation of *in vitro* CTA models is the use of immortalised cell lines, which may not be totally representative of the carcinogenic mechanisms existing in normal cells. Furthermore, rodent-based models, such as the Bhas 42 assay, cannot totally recapitulate the tumour development process of human cells [22]. In the future, the efficient risk assessment of NPL carcinogenicity will need to be based on the information collectively provided by several CTA models. In addition, transcriptomic analyses will allow elucidation of the molecular changes that occur during oncotransformation, which could be confirmed by integrating other *in vitro* assays targeting specific endpoints, such as the profile of inflammation-related interleukins and chemokines activated by the chemical exposure and/or the level and efficiency of cell-to-cell communications.

5. Conclusions

The objective of the current study was to assess the carcinogenic potential of two types of environmentally relevant secondary NPLs, PET and PLA, as well as pristine PS NPLs by using the regulatory assessment-approved *in vitro* Bhas 42 cell transformation assay. To the best of our knowledge, this is the first attempt to assess the tumourigenic potential of secondary NPLs; notably, the obtained results provide key information to support the carcinogenic risk assessment of these pollutants. Our findings showed that secondary PET NPLs can promote tumour progression, raising new questions regarding threshold concentrations in humans and potential synergies with co-exposed pollutants. The lack of cell-transforming capacity by the PS NPLs, despite previous evidence, illustrates the need to have well-characterised reference NPLs that will allow comparison between methods and the identification of key NPL properties that could affect their transforming capacity. In addition, future studies should aim at combining *in vitro* cell transformation models with the analyses of molecular changes and other *in vitro* assays targeting specific cancer-related endpoints to provide insights regarding the mechanisms underlying tumourigenesis. Finally, the new bioplastic PLA may be a safer alternative to other types of plastics, although further hazard assessment, including evaluation of other toxicological endpoints, is needed.

Environmental implications

Secondary nanoplastics (NPLs) generated from plastic waste degradation may bioaccumulate in human tissues and cause cancer. Currently, information regarding NPL carcinogenicity remains scarce. By using a regulatory assessment-accepted *in vitro* cell transformation assay, we assessed for the first time the carcinogenic potential of two secondary NPLs, polyethylene terephthalate and polylactic acid bioplastic, as examples of a widely spread waste plastic and a petroleum-based plastic alternative, respectively. Notably, the accelerated degradation of bioplastics has been associated with an enhanced release of NPLs into the environment. The generated data will serve to support the regulatory risk assessment of plastics.

CRediT authorship contribution statement

Aliro Villacorta: Writing – review & editing, Methodology, Formal analysis, Data curation. **Josefa Domenech:** Writing – review & editing, Writing – original draft, Methodology, Formal analysis, Data curation, Conceptualization. **Alba Hernández:** Writing – review & editing, Supervision, Funding acquisition. **Ricard Marcos:** Writing – review & editing, Supervision, Funding acquisition. **Raquel Llorens:** Resources. **Juan Francisco Ferrer:** Resources. **Julia Catalan:** Writing – review & editing, Writing – original draft, Visualization, Supervision, Project administration, Funding acquisition, Conceptualization.

Declaration of Competing Interest

The authors declare that they have no known competing financial interests or personal relationships that could have appeared to influence the work reported in this paper.

Data availability

Data will be made available on request.

Acknowledgment

Drs. Laurent Gaté, Yves Guichard and Caroline Vion are acknowledged for enabling J. Domenech to learn the Bhas 42 cell transformation assay at the Institut National de Recherche et de Sécurité pour la prévention des accidents du travail et des maladies professionnelles (INRS, France). The confocal microscopy facilities were outsourced to the Biomedicum Imaging Unit of the University of Helsinki.

A. Villacorta was supported by Ph.D. fellowships from the National Agency for Research and Development (ANID), from the CONICYT PFCHA/DOCTORADO BECAS CHILE/2020-72210237. A. Hernández was granted an ICREA ACADEMIA Award.

This project has received funding from the European Union's Horizon 2020 Research and Innovation Program under grant agreement No. 965196. This work was also partially supported by the Spanish Ministry of Science and Innovation [PID2020-116789, RB-C43], and by the Generalitat de Catalunya (2021-SGR-00731).

Appendix A. Supporting information

Supplementary data associated with this article can be found in the online version at doi:10.1016/j.jhazmat.2024.134030.

References

[1] Alaraby, M., Abass, D., Farre, M., Hernández, A., Marcos, R., 2024. Are bioplastics safe? Hazardous effects of polylactic acid (PLA) nanoplastics in Drosophila. Sci Total Environ 919, 170592. https://doi.org/10.1016/j.scitotenv.2024.170592.
[2] Alaraby, M., Villacorta, A., Abass, D., Hernández, A., Marcos, R., 2023. The hazardous impact of true-to-life PET nanoplastics in Drosophila. Sci Total Environ 863, 160954. https://doi.org/10.1016/j.scitotenv.2022.160954.
[3] Alaraby, M., Villacorta, A., Abass, D., Hernández, A., Marcos, R., 2024. Titanium-doped PET nanoplastics, from opaque milk bottle degradation, as a model of environmental true-to-life nanoplastics. Hazardous effects on Drosophila. Environ Pollut 341, 122968. https://doi.org/10.1016/j.envpol.2023.122968.
[4] Alzaben, M., Burve, R., Loeschner, K., Møller, P., Roursgaard, M., 2023. Nanoplastics from ground polyethylene terephthalate food containers: Genotoxicity in human lung epithelial A549 cells. Mutat Res Genet Toxicol Environ Mutagen 892, 503705. https://doi.org/10.1016/j.mrgentox.2023.503705.
[5] Amereh, F., Babaei, M., Eslami, A., Fazelipour, S., Rafiee, M., 2020. The emerging risk of exposure to nano(micro)plastics on endocrine disturbance and reproductive toxicity: from a hypothetical scenario to a global public health challenge. Environ Pollut 261, 114158. https://doi.org/10.1016/j.envpol.2020.114158.
[6] An, R., Wang, X., Yang, L., Zhang, J., Wang, N., Xu, F., et al., 2021. Polystyrene microplastics cause granulosa cells apoptosis and fibrosis in ovary through oxidative stress in rats. Toxicology 449, 152665. https://doi.org/10.1016/j.tox.2020.152665.
[7] Annangi, B., Villacorta, A., Vela, L., Tavakolpournegari, A., Marcos, R., Hernández, A., 2023. Effects of true-to-life PET nanoplastics using primary human nasal epithelial cells. Environ Toxicol Pharm 100, 104140. https://doi.org/10.1016/j.etap.2023.104140.
[8] AOP-Wiki; 2023. AOP-Wiki. https://aopwiki.org/aops (Accessed December 2023).
[9] Asada, S., Sasaki, K., Tanaka, N., Takeda, K., Hayashi, M., Umeda, M., 2005. Detection of initiating as well as promoting activity of chemicals by a novel cell transformation assay using v-Ha-ras-transfected BALB/c 3T3 cells (Bhas 42 cells). Mutat Res/Genet Toxicol Environ Mutagen 588 (1), 7–21. https://doi.org/10.1016/j.mrgentox.2005.07.011.
[10] Ballesteros, S., Domenech, J., Barguilla, I., Cortés, C., Marcos, R., Hernández, A., 2020. Genotoxic and immunomodulatory effects in human white blood cells after ex vivo exposure to polystyrene nanoplastics [10.1039/D0EN00748J]. Environ Sci: Nano 7 (11), 3431–3446. https://doi.org/10.1039/D0EN00748J.
[11] Banaei, G., García-Rodríguez, A., Tavakolpournegari, A., Martín-Pérez, J., Villacorta, A., Marcos, R., et al., 2023. The release of polylactic acid nanoplastics (PLA-NPLs) from commercial teabags. Obtention, characterization, and hazard effects of true-to-life PLA-NPLs. J Hazard Mater 458, 131899. https://doi.org/10.1016/j.jhazmat.2023.131899.
[12] Barbosa, F., Adeyemi, J.A., Bocato, M.Z., Comas, A., Campiglia, A., 2020. A critical viewpoint on current issues, limitations, and future research needs on micro- and nanoplastic studies: from the detection to the toxicological assessment. Environ Res 182, 109089. https://doi.org/10.1016/j.envres.2019.109089.
[13] Barguilla, I., Domenech, J., Ballesteros, S., Rubio, L., Marcos, R., Hernández, A., 2022. Long-term exposure to nanoplastics alters molecular and functional traits related to the carcinogenic process. J Hazard Mater 438, 129470. https://doi.org/10.1016/j.jhazmat.2022.129470.
[14] Barguilla, I., Domenech, J., Rubio, L., Marcos, R., Hernández, A., 2022. Nanoplastics and arsenic co-exposures exacerbate oncogenic biomarkers under an in vitro long-term exposure scenario. Int J Mol Sci 23 (6). https://doi.org/10.3390/ijms23062958.
[15] Barguilla, I., Maguer-Satta, V., Guyot, B., Pastor, S., Marcos, R., Hernández, A., 2023. In vitro approaches to determine the potential carcinogenic risk of environmental pollutants. Int J Mol Sci 24 (9). https://doi.org/10.3390/ijms24097851.
[16] Bhattacharjee, S., 2016. DLS and zeta potential - what they are and what they are not? J Control Release 235, 337–351. https://doi.org/10.1016/j.jconrel.2016.06.017.

[17] Bioplastics E. Bioplastics market development update 2023; 2023. Retrieved 2/24/2024 from https://www.european-bioplastics.org/market/.

[18] Bonanomi, M., Salmistraro, N., Porro, D., Pinsino, A., Colangelo, A.M., Gaglio, D., 2022. Polystyrene micro and nano-particles induce metabolic rewiring in normal human colon cells: A risk factor for human health. Chemosphere 303, 134947. https://doi.org/10.1016/j.chemosphere.2022.134947.

[19] Cássio, F., Batista, D., Pradhan, A., 2022. Plastic interactions with pollutants and consequences to aquatic ecosystems: what we know and what we do not know. Biomolecules 12 (6), 798. ⟨https://www.mdpi.com/2218-273X/12/6/798⟩.

[20] Catalán, J., Stockmann-Juvala, H., Norppa, H., 2017. A theoretical approach for a weighted assessment of the mutagenic potential of nanomaterials. Nanotoxicology 11 (8), 964–977. https://doi.org/10.1080/17435390.2017.1382601.

[21] Chandler, C., Liu, T., Buckanovich, R., Coffman, L.G., 2019. The double edge sword of fibrosis in cancer. Transl Res 209, 55–67. https://doi.org/10.1016/j.trsl.2019.02.006.

[22] Chatterjee, N., Alfaro-Moreno, E., 2023. In vitro cell transformation assays: a valuable approach for carcinogenic potentiality assessment of nanomaterials. Int J Mol Sci 24 (9). https://doi.org/10.3390/ijms24098219.

[23] Chen, G., Shan, H., Xiong, S., Zhao, Y., van Gestel, C.A.M., Qiu, H., et al., 2024. Polystyrene nanoparticle exposure accelerates ovarian cancer development in mice by altering the tumor microenvironment. Sci Total Environ 906, 167592. https://doi.org/10.1016/j.scitotenv.2023.167592.

[24] Colacci, A., Corvi, R., Ohmori, K., Paparella, M., Serra, S., Da Rocha Carrico, I., et al., 2023. The cell transformation assay: a historical assessment of current knowledge of applications in an integrated approach to testing and assessment for non-genotoxic carcinogens. Int J Mol Sci 24 (6). https://doi.org/10.3390/ijms24065659.

[25] Cox, K.D., Covernton, G.A., Davies, H.L., Dower, J.F., Juanes, F., Dudas, S.E., 2019. Human consumption of microplastics. Environ Sci Technol 53 (12), 7068–7074. https://doi.org/10.1021/acs.est.9b01517.

[26] Deng, J., Ibrahim, M.S., Tan, L.Y., Yeo, X.Y., Lee, Y.A., Park, S.J., et al., 2022. Microplastics released from food containers can suppress lysosomal activity in mouse macrophages. J Hazard Mater 435, 128980. https://doi.org/10.1016/j.jhazmat.2022.128980.

[27] Domenech, J., Annangi, B., Marcos, R., Hernández, A., Catalán, J., 2023. Insights into the potential carcinogenicity of micro- and nano-plastics. Mutat Res/Rev Mutat Res 791, 108453. https://doi.org/10.1016/j.mrrev.2023.108453.

[28] Domenech, J., Marcos, R., 2021. Pathways of human exposure to microplastics, and estimation of the total burden. Curr Opin Food Sci 39, 144–151. https://doi.org/10.1016/j.cofs.2021.01.004.

[29] EC. EUROPEAN COMMISSION RECOMMENDATION of 10 June 2022 on the definition of nanomaterial; 2022. Retrieved from https://eur-lex.europa.eu/legal-content/EN/TXT/PDF/?uri=CELEX:32022H0614(01).

[30] ECHA. Report on the European Chemicals Agency's "New Approach Methodologies Workshop: Towards an Animal Free Regulatory System for Industrial Chemicals" 31 May – 1 June 2023, Helsinki, Finland. E. C. Agency; 2023. https://echa.europa.eu/documents/10162/17220/nams_ws_june2023_en.pdf/06b8bc28-c563–3a36-cfa9–0fa5453b88a7?t=1695620290072.

[31] Europe P. Plastics - The fast Facts 2023; 2023. Retrieved 2/24/2024 from https://plasticseurope.org/wp-content/uploads/2023/10/Plasticsthefastfacts2023–1.pdf.

[32] Facciolà, A., Visalli, G., Pruiti Ciarello, M., Di Pietro, A., 2021. Newly emerging airborne pollutants: current knowledge of health impact of micro and nanoplastics. Int J Environ Res Public Health 18 (6).

[33] Fang, J., Xuan, Y., Li, Q., 2010. Preparation of polystyrene spheres in different particle sizes and assembly of the PS colloidal crystals. Sci China Technol Sci 53 (11), 3088–3093. https://doi.org/10.1007/s11431-010-4110-5.

[34] Fojt, J., David, J., Přikryl, R., Řezáčová, V., Kučerík, J., 2020. A critical review of the overlooked challenge of determining micro-bioplastics in soil. Sci Total Environ 745, 140975. https://doi.org/10.1016/j.scitotenv.2020.140975.

[35] Fontana, C., Kirsch, A., Seidel, C., Marpeaux, L., Darne, C., Gaté, L., et al., 2017. In vitro cell transformation induced by synthetic amorphous silica nanoparticles. Mutat Res Genet Toxicol Environ Mutagen 823, 22–27. https://doi.org/10.1016/j.mrgentox.2017.08.002.

[36] Forte, M., Iachetta, G., Tussellino, M., Carotenuto, R., Prisco, M., De Falco, M., et al., 2016. Polystyrene nanoparticles internalization in human gastric adenocarcinoma cells. Toxicol Vitr 31, 126–136. https://doi.org/10.1016/j.tiv.2015.11.006.

[37] Gábelová, A., El Yamani, N., Alonso, T.I., Buliaková, B., Srančíková, A., Bábelová, A., et al., 2017. Fibrous shape underlies the mutagenic and carcinogenic potential of nanosilver while surface chemistry affects the biosafety of iron oxide nanoparticles. Mutagenesis 32 (1), 193–202. https://doi.org/10.1093/mutage/gew045.

[38] Ghafouri-Fard, S., Khoshbakht, T., Hussen, B.M., Dong, P., Gassler, N., Taheri, M., et al., 2022. A review on the role of cyclin dependent kinases in cancers. Cancer Cell Int 22 (1), 325. https://doi.org/10.1186/s12935-022-02747-z.

[39] Guichard, Y., Savoy, C., Gaté, L., 2023. Can a 12-gene expression signature predict the cell transforming potential of tumor promoting agents in Bhas 42 cells? Toxicol Lett 389, 11–18. https://doi.org/10.1016/j.toxlet.2023.10.006.

[40] Hayrapetyan, R., Lacour, T., Luce, A., Finot, F., Chagnon, M.C., Séverin, I., 2023. The cell transformation assay to assess potential carcinogenic properties of nanoparticles. Mutat Res Rev Mutat Res 791, 108455. https://doi.org/10.1016/j.mrrev.2023.108455.

[41] Hernandez, L.M., Xu, E.G., Larsson, H.C.E., Tahara, R., Maisuria, V.B., Tufenkji, N., 2019. Plastic teabags release billions of microparticles and nanoparticles into tea. Environ Sci Technol 53 (21), 12300–12310. https://doi.org/10.1021/acs.est.9b02540.

[42] Hodges, N.J., Adám, B., Lee, A.J., Cross, H.J., Chipman, J.K., 2001. Induction of DNA-strand breaks in human peripheral blood lymphocytes and A549 lung cells by sodium dichromate: association with 8-oxo-2-deoxyguanosine formation and inter-individual variability. Mutagenesis 16 (6), 467–474. https://doi.org/10.1093/mutage/16.6.467.

[43] Jacobs, M.N., Colacci, A., Corvi, R., Vaccari, M., Aguila, M.C., Corvaro, M., et al., 2020. Chemical carcinogen safety testing: OECD expert group international consensus on the development of an integrated approach for the testing and assessment of chemical non-genotoxic carcinogens. Arch Toxicol 94 (8), 2899–2923. https://doi.org/10.1007/s00204-020-02784-5.

[44] Jagiello K, Sosnowska A, Stępnik M, Gromelski M, Płonka K. Nano-specific alternative methods in human hazard/safety assessment under different EU regulations, considering the animal testing bans already in place for cosmetics and their ingredients. E. U. O. f. Nanomaterials2022. https://euon.echa.europa.eu/documents/2435000/3268573/ECHA-62–2022_final_report_published_02aug2023.pdf/4071837e-c4de-b496-b00f-4e5317646713?t=1691138948441.

[45] Jasinski, J., Völkl, M., Wilde, M.V., Jérôme, V., Fröhlich, T., Freitag, R., et al., 2024. Influence of the polymer type of a microplastic challenge on the reaction of murine cells. J Hazard Mater 465, 133280. https://doi.org/10.1016/j.jhazmat.2023.133280.

[46] Jensen KA. Standard operating procedures for characterisation of the selected MN types; 2011. https://www.anses.fr/en/system/files/nanogenotox_deliverable_5.pdf.

[47] Jeon, S., Jeon, J.H., Jeong, J., Kim, G., Lee, S., Kim, S., et al., 2023. Size- and oxidative potential-dependent toxicity of environmentally relevant expanded polystyrene styrofoam microplastics to macrophages. J Hazard Mater 459, 132295. https://doi.org/10.1016/j.jhazmat.2023.132295.

[48] Jin, Y.J., Kim, J.E., Roh, Y.J., Song, H.J., Seol, A., Park, J., et al., 2023. Characterisation of changes in global genes expression in the lung of ICR mice in response to the inflammation and fibrosis induced by polystyrene nanoplastics inhalation. Toxicol Res 39 (4), 1–25. https://doi.org/10.1007/s43188-023-00188-y.

[49] Johnson, L.M., Mecham, J.B., Krovi, S.A., Moreno Caffaro, M.M., Aravamudhan, S., Kovach, A.L., et al., 2021. Fabrication of polyethylene terephthalate (PET) nanoparticles with fluorescent tracers for studies in mammalian cells [10.1039/D0NA00888E]. Nanoscale Adv 3 (2), 339–346. https://doi.org/10.1039/D0NA00888E.

[50] Kim, H., Zaheer, J., Choi, E.-J., Kim, J.S., 2022. Enhanced ASGR2 by microplastic exposure leads to resistance to therapy in gastric cancer [Research Paper]. Theranostics 12 (7), 3217–3236. https://doi.org/10.7150/thno.73226.

[51] Kirsch, A., Dubois-Pot-Schneider, H., Fontana, C., Schohn, H., Gaté, L., Guichard, Y., 2020. Predictive early gene signature during mouse Bhas 42 cell transformation induced by synthetic amorphous silica nanoparticles. Chem Biol Inter 315, 108900. https://doi.org/10.1016/j.cbi.2019.108900.

[52] Kortenkamp, A., Faust, M., Scholze, M., Backhaus, T., 2007. Low-level exposure to multiple chemicals: reason for human health concerns? Environ Health Perspect 115 (Suppl 1), 106–114. https://doi.org/10.1289/ehp.9358.

[53] Kumar, R., Manna, C., Padha, S., Verma, A., Sharma, P., Dhar, A., et al., 2022. Micro(nano)plastics pollution and human health: How plastics can induce carcinogenesis to humans? Chemosphere 298, 134267. https://doi.org/10.1016/j.chemosphere.2022.134267.

[54] Le, V.-G., Nguyen, M.-K., Nguyen, H.-L., Lin, C., Hadi, M., Hung, N.T.Q., et al., 2023. A comprehensive review of micro- and nano-plastics in the atmosphere: Occurrence, fate, toxicity, and strategies for risk reduction. Sci Total Environ 904, 166649. https://doi.org/10.1016/j.scitotenv.2023.166649.

[55] Leslie, H.A., van Velzen, M.J.M., Brandsma, S.H., Vethaak, A.D., Garcia-Vallejo, J. J., Lamoree, M.H., 2022. Discovery and quantification of plastic particle pollution in human blood. Environ Int 163, 107199. https://doi.org/10.1016/j.envint.2022.107199.

[56] Li, L., Xu, M., He, C., Wang, H., Hu, Q., 2022. Polystyrene nanoplastics potentiate the development of hepatic fibrosis in high fat diet fed mice. Environ Toxicol 37 (2), 362–372. https://doi.org/10.1002/tox.23404.

[57] Liang, B., Zhong, Y., Huang, Y., Lin, X., Liu, J., Lin, L., et al., 2021. Underestimated health risks: polystyrene micro- and nanoplastics jointly induce intestinal barrier dysfunction by ROS-mediated epithelial cell apoptosis. Part Fibre Toxicol 18 (1), 20. https://doi.org/10.1186/s12989-021-00414-1.

[58] Lin, P., Tong, X., Xue, F., Qianru, C., Xinyu, T., Zhe, L., et al., 2022. Polystyrene nanoplastics exacerbate lipopolysaccharide-induced myocardial fibrosis and autophagy in mice via ROS/TGF-β1/Smad. Toxicology 480, 153338. https://doi.org/10.1016/j.tox.2022.153338.

[59] Miller, D.M., Thomas, S.D., Islam, A., Muench, D., Sedoris, K., 2012. c-Myc and cancer metabolism. Clin Cancer Res 18 (20), 5546–5553. https://doi.org/10.1158/1078-0432.Ccr-12-0977.

[60] Mulcahy Levy, J.M., Thorburn, A., 2020. Autophagy in cancer: moving from understanding mechanism to improving therapy responses in patients. Cell Death Differ 27 (3), 843–857. https://doi.org/10.1038/s41418-019-0474-7.

[61] Møller, P., Roursgaard, M., 2023. Exposure to nanoplastic particles and DNA damage in mammalian cells. Mutat Res Rev Mutat Res 792, 108468. https://doi.org/10.1016/j.mrrev.2023.108468.

[62] Nazrin, A., Sapuan, S.M., Zuhri, M.Y.M., 2020. Mechanical, physical and thermal properties of sugar palm nanocellulose reinforced thermoplastic starch (TPS)/Poly (Lactic Acid) (PLA) Blend Bionanocomposites. Polymers (Basel) 12 (10). https://doi.org/10.3390/polym12102216.

[63] OECD. Guidance Document on the in Vitro Bhas 42 Cell Transformation Assay. Organisation for Economic Co-operation and Development; 2017. https://one.oecd.org/document/ENV/JM/MONO(2016)1/en/pdf.

[64] Prata, J.C., 2018. Airborne microplastics: consequences to human health? Environ Pollut 234, 115–126. https://doi.org/10.1016/j.envpol.2017.11.043.
[65] Prata, J.C., da Costa, J.P., Lopes, I., Duarte, A.C., Rocha-Santos, T., 2020. Environmental exposure to microplastics: An overview on possible human health effects. Sci Total Environ 702, 134455. https://doi.org/10.1016/j.scitotenv.2019.134455.
[66] Ramsperger, A.F.R.M., Bergamaschi, E., Panizzolo, M., Fenoglio, I., Barbero, F., Peters, R., et al., 2023. Nano- and microplastics: a comprehensive review on their exposure routes, translocation, and fate in humans. NanoImpact 29, 100441. https://doi.org/10.1016/j.impact.2022.100441.
[67] Rist, S., Carney Almroth, B., Hartmann, N.B., Karlsson, T.M., 2018. A critical perspective on early communications concerning human health aspects of microplastics. Sci Total Environ 626, 720–726. https://doi.org/10.1016/j.scitotenv.2018.01.092.
[68] Roursgaard, M., Hezareh Rothmann, M., Schulte, J., Karadimou, I., Marinelli, E., Møller, P., 2022. Genotoxicity of particles from grinded plastic items in Caco-2 and HepG2 Cells [Original Research]. Front Public Health 10. https://doi.org/10.3389/fpubh.2022.906430.
[69] Rubio, L., Barguilla, I., Domenech, J., Marcos, R., Hernández, A., 2020. Biological effects, including oxidative stress and genotoxic damage, of polystyrene nanoparticles in different human hematopoietic cell lines. J Hazard Mater 398, 122900. https://doi.org/10.1016/j.jhazmat.2020.122900.
[70] Sakai, A., Sasaki, K., Muramatsu, D., Arai, S., Endou, N., Kuroda, S., et al., 2010. A Bhas 42 cell transformation assay on 98 chemicals: the characteristics and performance for the prediction of chemical carcinogenicity. Mutat Res/Genet Toxicol Environ Mutagen 702 (1), 100–122. https://doi.org/10.1016/j.mrgentox.2010.07.007.
[71] Senathirajah, K., Attwood, S., Bhagwat, G., Carbery, M., Wilson, S., Palanisami, T., 2021. Estimation of the mass of microplastics ingested – a pivotal first step towards human health risk assessment. J Hazard Mater 404, 124004. https://doi.org/10.1016/j.jhazmat.2020.124004.
[72] Shi, Q., Tang, J., Wang, L., Liu, R., Giesy, J.P., 2021. Combined cytotoxicity of polystyrene nanoplastics and phthalate esters on human lung epithelial A549 cells and its mechanism. Ecotoxicol Environ Saf 213, 112041. https://doi.org/10.1016/j.ecoenv.2021.112041.
[73] Siivola, K.M., Burgum, M.J., Suárez-Merino, B., Clift, M.J.D., Doak, S.H., Catalán, J., 2022. A systematic quality evaluation and review of nanomaterial genotoxicity studies: a regulatory perspective. Part Fibre Toxicol 19 (1), 59. https://doi.org/10.1186/s12989-022-00499-2.
[74] Statista. Global plastic waste generation outlook 2020–2060; 2024. Retrieved 2/24/2024 from https://www.statista.com/statistics/1338839/global-plastic-waste-generation-outlook/.
[75] Strupp, C., Corvaro, M., Cohen, S.M., Corton, J.C., Ogawa, K., Richert, L., et al., 2023. Increased cell proliferation as a key event in chemical carcinogenesis: application in an integrated approach for the testing and assessment of non-genotoxic carcinogenesis. Int J Mol Sci 24 (17). https://doi.org/10.3390/ijms241713246.
[76] Sun, A., Wang, W.-X., 2023. Human exposure to microplastics and its associated health risks. Environ Health 1 (3), 139–149. https://doi.org/10.1021/envhealth.3c00053.
[77] Uboldi, C., Urbán, P., Gilliland, D., Bajak, E., Valsami-Jones, E., Ponti, J., et al., 2016. Role of the crystalline form of titanium dioxide nanoparticles: rutile, and not anatase, induces toxic effects in Balb/3T3 mouse fibroblasts. Toxicol Vitr 31, 137–145. https://doi.org/10.1016/j.tiv.2015.11.005.
[78] Villacorta, A., Rubio, L., Alaraby, M., López-Mesas, M., Fuentes-Cebrian, V., Moriones, O.H., et al., 2022. A new source of representative secondary PET nanoplastics. Obtention, characterization, and hazard evaluation. J Hazard Mater 439, 129593. https://doi.org/10.1016/j.jhazmat.2022.129593.
[79] Wang, M., Li, Q., Shi, C., Lv, J., Xu, Y., Yang, J., et al., 2023. Oligomer nanoparticle release from polylactic acid plastics catalysed by gut enzymes triggers acute inflammation. Nat Nanotechnol 18 (4), 403–411. https://doi.org/10.1038/s41565-023-01329-y.
[80] Wieland, S., Balmes, A., Bender, J., Kitzinger, J., Meyer, F., Ramsperger, A.F.R.M., et al., 2022. From properties to toxicity: Comparing microplastics to other airborne microparticles. J Hazard Mater 428, 128151. https://doi.org/10.1016/j.jhazmat.2021.128151.
[81] Xu, M., Halimu, G., Zhang, Q., Song, Y., Fu, X., Li, Y., et al., 2019. Internalization and toxicity: a preliminary study of effects of nanoplastic particles on human lung epithelial cell. Sci Total Environ 694, 133794. https://doi.org/10.1016/j.scitotenv.2019.133794.
[82] Yadav, H., Sethulekshmi, S., Shriwastav, A., 2022. Estimation of microplastic exposure via the composite sampling of drinking water, respirable air, and cooked food from Mumbai, India. Environ Res 214 (Pt 1), 113735. https://doi.org/10.1016/j.envres.2022.113735.
[83] Yang, Q., Dai, H., Wang, B., Xu, J., Zhang, Y., Chen, Y., et al., 2023. Nanoplastics Shape Adaptive Anticancer Immunity in the Colon in Mice. Nano Lett 23 (8), 3516–3523. https://doi.org/10.1021/acs.nanolett.3c00644.
[84] Yang, Z., DeLoid, G.M., Zarbl, H., Baw, J., Demokritou, P., 2023. Micro- and nanoplastics (MNPs) and their potential toxicological outcomes: State of science, knowledge gaps and research needs. NanoImpact 32, 100481. https://doi.org/10.1016/j.impact.2023.100481.
[85] Zambrano-Pinto, M.V., Tinizaray-Castillo, R., Riera, M.A., Maddela, N.R., Luque, R., Díaz, J.M.R., 2024. Microplastics as vectors of other contaminants: analytical determination techniques and remediation methods. Sci Total Environ 908, 168244. https://doi.org/10.1016/j.scitotenv.2023.168244.